A BDOPV-Based Donor–Acceptor Polymer for High-Performance n-Type and Oxygen-Doped Ambipolar Field-Effect Transistors

Ting Lei, Jin-Hu Dou, Xiao-Yu Cao, Jie-Yu Wang,* and Jian Pei**

Due to their solution processability and mechanical robustness, semiconducting polymers have been widely used for high-throughput production of low-cost, light-weight, and flexible devices.[1] A powerful strategy to achieve high carrier mobilities in semiconducting polymers is the development of an alternating conjugated polymer containing electron-rich (donor) and electron-deficient (acceptor) units.[2] Because of their successful application in high-performance organic field-effect transistors (OFETs) and organic photovoltaics (OPVs), these donor–acceptor polymers were named third-generation polymers by Heeger.[3] Recently, electron-deficient fused aromatic rings such as diketopyrrolopyrrole (DPP),[4] benzothiadiazole (BT),[5] isoindigo (II),[6] naphthalene diimide (NDI),[7] and benzobisthiadiazole (BBT)[8] have been used as acceptors to construct donor–acceptor polymers, leading to the significant development of polymer FETs. High hole mobilities over 10 $cm^2\ V^{-1}\ s^{-1}$ under ambient conditions and electron mobilities over 1 $cm^2\ V^{-1}\ s^{-1}$ in inert atmosphere have been achieved.[9] Nevertheless, very few n-type polymers are known to operate under ambient conditions,[10] and they generally exhibit electron mobilities lower than 1 $cm^2\ V^{-1}\ s^{-1}$. Moreover, oxygen (even short-time exposure) can significantly degrade the device performance of these n-type FETs.[11]

Two methods are generally used to improve electron mobility and device stability in polymer FETs: 1) lower the LUMO level to stabilize electron transport and 2) enlarge the intermolecular overlaps of LUMOs to facilitate electron hopping.[12] Using both methods, we recently developed a new electron-deficient building block benzodifurandione-based oligo(*p*-phenylene vinylene) (**BDOPV**), regarded as a derivative of oligo(*p*-phenylene vinylene) (**Scheme 1**).[13] In **BDOPV**, four carbonyl groups were introduced to give a low LUMO level of –4.24 eV. Furthermore, these carbonyl groups formed four intramolecular hydrogen bonds with the neighboring phenyl protons, maintaining good planarity and shape-persistency of **BDOPV**, which may facilitate the overlap of intermolecular frontier orbitals of the **BDOPV** segments in polymers. Indeed, a second-generation polymer benzodifurandione-based poly(p-phenylene vinylene) (**BDPPV**) based on **BDOPV** provided remarkably high electron mobilities up to 1.1 $cm^2\ V^{-1}\ s^{-1}$ under ambient conditions.[13]

Previously, we significantly increased hole mobilities of II-based polymers by using longer branched alkyl chains[14] or centrosymmetric donors (versus axisymmetric donors).[15] Herein, we incorporate all the strategies by using the **BDOPV** unit as the acceptor, a long branched 4-octadecyldocosyl group as the side chain, and a centrosymmetric 2,2′-bithiophene unit as the donor to synthesize donor–acceptor polymer **BDOPV-2T**, a typical third-generation polymer (Scheme 1).[16] To our delight, **BDOPV-2T** exhibits n-type transport behavior with high electron mobilities up to 1.74 $cm^2\ V^{-1}\ s^{-1}$ under ambient conditions. Upon oxygen exposure, this polymer displays interesting ambipolar transporting behavior, which maintains high electron mobilities up to 1.45 $cm^2\ V^{-1}\ s^{-1}$, along with significantly increased hole mobilities up to 0.47 $cm^2\ V^{-1}\ s^{-1}$. To our knowledge, these electron mobilities are among the highest in polymer FETs, and our work represents the first polymer exhibiting electron mobilities over 1 $cm^2\ V^{-1}\ s^{-1}$ for devices fabricated under ambient conditions.

As illustrated in Scheme 1, **BDOPV** was synthesized from 2,2′-(2,5-dihydroxy-1,4-phenylene)diacetic acid (**1**) in two steps with moderate yield.[13] Note that different functional groups can be readily introduced on compound **3** to give other **BDOPV**s, thus providing a facile route to modulate the electronic properties of **BDOPV**. A Stille coupling polymerization between **BDOPV** and 5,5′-bis(trimethylstannyl)-2,2′-bithiophene gave polymer **BDOPV-2T** in 94% yield after standard purification. The molecular weight of **BDOPV-2T** was evaluated by high-temperature gel permeation chromatography at 140 °C using 1,2,4-tricholorobenzene as the eluent. The polymer displayed a high molecular weight with an $\overline{M}_n$ of 77.2 kDa and a polydispersity index (PDI) of 3.00, and excellent thermal stability with a decomposition temperature over 390 °C (Figures S1 and S2, Supporting Information).

The absorption spectra of polymer **BDOPV-2T** in dilute solution, thin film, and annealed film are shown in **Figure 1**a. **BDOPV-2T** showed typical dual-band absorption, where Band I is a typical charge transfer absorption from the thiophene unit to the **BDOPV** core, because computational results showed that its HOMO was well delocalized along the polymer chain; in contrast, its LUMO was mostly localized on the **BDOPV** cores (Figure 1b). The absorption maximum of **BDOPV-2T** in a film

T. Lei, J.-H. Dou, Dr. J.-Y. Wang, Prof. J. Pei
Beijing National Laboratory for Molecular Sciences
The Key Laboratory of Bioorganic Chemistry
and Molecular Engineering of Ministry of Education
College of Chemistry and Molecular Engineering
Peking University
Beijing, 100871, China
E-mail: jieyuwang@pku.edu.cn; jianpei@pku.edu.cn
Prof. X.-Y. Cao
College of Chemistry and Chemical Engineering
Xiamen University
Xiamen, 361005, China
E-mail: xcao@xmu.edu.cn

DOI: 10.1002/adma.201302278

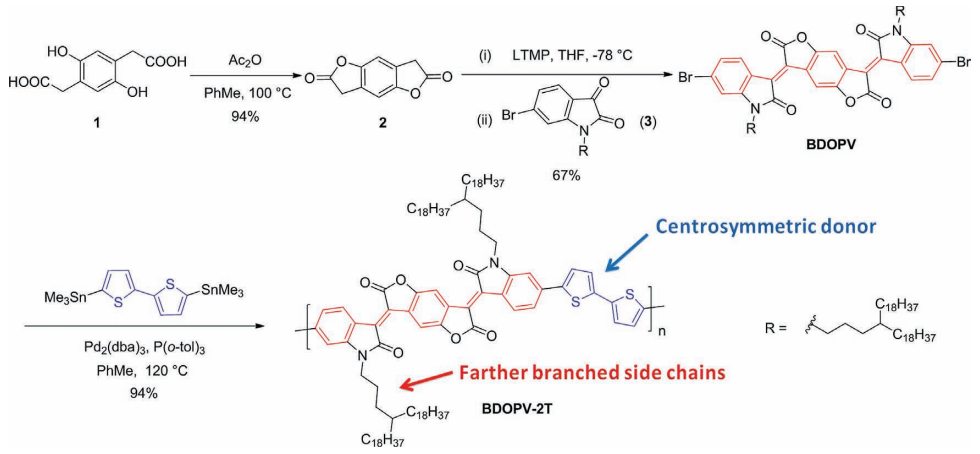

Scheme 1. Design and synthesis of polymer **BDOPV-2T**.

only showed a minimal red-shift in comparison to that in the solution, and a slight increase of the 0–0 vibrational peak was observed. Annealing the film led to a further increase of the 0–0 peak. These results indicate that the polymer backbone in the film becomes more planar and annealing is helpful for a further adjustment of the polymer backbone. The bandgap of **BDOPV-2T** is calculated to be 1.31 eV using the onset of its thin-film absorption spectrum. The cyclic voltammetry (CV) measurement of **BDOPV-2T** gave HOMO/LUMO levels of –5.72/–4.15 eV, consistent with the HOMO/LUMO levels (–5.66/–4.35 eV) estimated from photoelectron spectroscopy and the optical bandgap (Table S1 and Figure S3). Note that this LUMO level is significantly lower than those of many previously reported donor–acceptor polymers,[2a,b] due to the strong electron-withdrawing ability of the **BDOPV** moiety.

The low-lying LUMO level of polymer **BDOPV-2T** indicates that it is perhaps suitable for ambient-stable electron transport. To achieve this goal, a top-gate/bottom-contact (TG/BC) device configuration was used to fabricate polymer FETs, because this device configuration has better injection characteristics and encapsulation effects.[17] The semiconducting layer was deposited by spin-coating the polymer solution (3 mg mL^{-1} in 1,2-dichlorobenzene (DCB)) on a patterned $n^{++}Si/SiO_2/Au$ (source–drain) substrate. After thermally annealing the film for 5 min, a CYTOP solution was spin-coated as the dielectric layer, and an aluminum layer was thermally evaporated as the gate electrode. Except for the aluminum layer which was deposited under high vacuum, we fabricated the devices either in a glovebox or under ambient conditions. Several annealing temperatures were performed, and annealing at 200 °C gave the best device performance (Table S2). All devices were tested under ambient conditions (relative humidity, R_H = 40–50%). For devices fabricated in a glovebox, **BDOPV-2T** displayed clearly n-type transport characteristics (**Figure 2**a and 2b), with high electron mobilities up to 1.74 $cm^2\ V^{-1}\ s^{-1}$ and an average mobility of 1.42 $cm^2\ V^{-1}\ s^{-1}$, which is the highest electron mobility for polymer FETs tested under ambient conditions.

For devices fabricated under ambient conditions, the hole mobilities of **BDOPV-2T** significantly increased. The highest hole mobility of 0.47 $cm^2\ V^{-1}\ s^{-1}$ and an average mobility of 0.20 $cm^2\ V^{-1}\ s^{-1}$ were obtained. In contrast, the highest electron mobility of **BDOPV-2T** only slightly decreased to 1.45 $cm^2\ V^{-1}\ s^{-1}$ (average: 1.20 $cm^2\ V^{-1}\ s^{-1}$) (Figure 2c and 2d). Note that the transfer characteristics of electron transport showed negligible hysteresis even at a low drain voltage (V_D = + 20 V), presumably due to the much lowered LUMO level of **BDOPV-2T**. Moreover, devices fabricated under ambient conditions displayed a larger threshold voltage in n-channel operation,

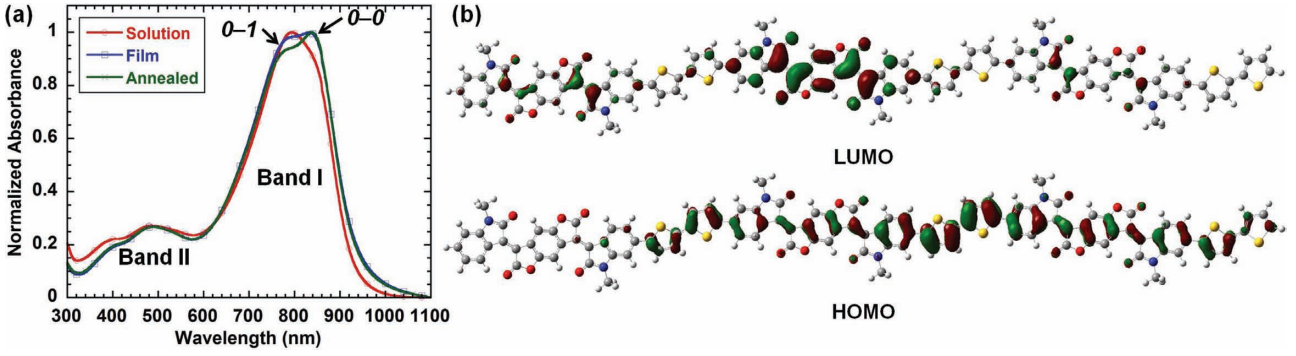

Figure 1. a) Normalized absorption spectra of **BDOPV-2T** in $CHCl_3$ (1×10^{-5} M), thin film, and annealed film (200 °C for 5 min). b) Calculated molecular orbitals of the trimer of **BDOPV-2T** (B3LYP/6-311G(d,p)).

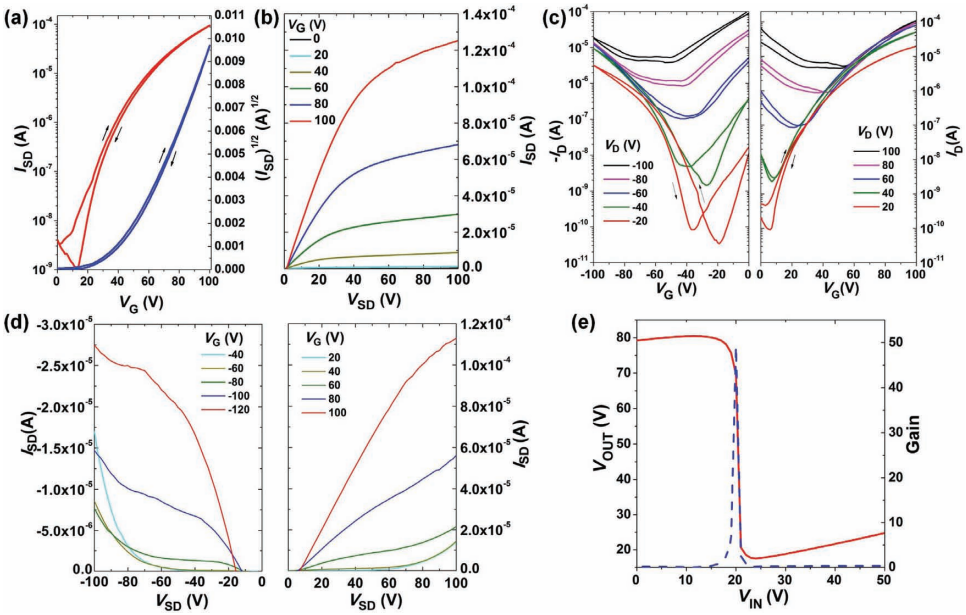

Figure 2. a) Transfer and b) output characteristics of a **BDOPV-2T** device fabricated in a glovebox and tested under ambient conditions. c) Transfer and d) output characteristics of a **BDOPV-2T** device both fabricated and tested under ambient conditions. Device configuration: TG/BC, $L = 5\,\mu m$, $W = 100\,\mu m$, $C_i = 3.7$ nF cm^{-2}. e) The voltage transfer characteristic and gain of a complementary-like inverter fabricated with **BDOPV-2T** under ambient conditions.

suggesting some kinds of shallow traps were formed in the film. To further explore the application of this ambipolar FET, we also fabricated complementary-like inverters based on polymer **BDOPV-2T** under ambient conditions. The inverter consisted of two connected TG/BC ambipolar transistors with a common gate as input (V_{IN}) and a common drain as output (V_{OUT}). Obviously inverting functionality was observed for the inverter based on **BDOPV-2T**, and the highest gain value up to 49 was obtained (Figure 2e). This gain value is also among the highest in ambipolar FETs.[18]

Time-dependent decay of the polymer devices was measured by exposing the devices to air in a desiccator or under ambient conditions (R_H = 40–50%). Devices under both conditions did not show any obvious difference, suggesting that water has negligible effects on the device performance. For devices fabricated in a glovebox, we observed a gradual decay of electron mobilities and an increase of hole mobilities (Figure S4). After one day exposure, the electron mobilities dropped to around 1 cm^2 V^{-1} s^{-1} and the hole mobilities increased from 10^{-2} to around 0.1 cm^2 V^{-1} s^{-1}. The device performance is comparable to those of the devices fabricated under ambient conditions. Prolonged storage in air led to a further decrease of electron mobilities. After 15 days, an electron mobility of 0.35 cm^2 V^{-1} s^{-1} and a hole mobility of 0.15 cm^2 V^{-1} s^{-1} were obtained. Thus, we propose that the significantly increased hole mobilities for **BDOPV-2T** devices fabricated under ambient conditions were largely attributed to the oxygen doping in the polymer film.

Oxygen doping has been widely investigated in inorganic materials, which has a strong influence on their electrical characteristics.[19] Recently, a p-type small molecule, picene, was reported to have a much higher hole mobility in air than in vacuum.[20] In this system, the energy levels of the highest three occupied molecular orbitals apparently increased after exposing to oxygen, leading to the inactivation of hole traps and the reduction of the hole injection barrier.[21] To understand the oxygen doping on a molecular level, we performed density functional theory (DFT) calculations to model the interaction between oxygen and **BDOPV-2T** (**Figure 3**). We found that the oxygen and **BDOPV-2T** formed a stable complex through van der Waals interactions. The complex exhibited a lower LUMO level and the LUMO clearly delocalized onto the oxygen. These results are in agreement with the device performance that some

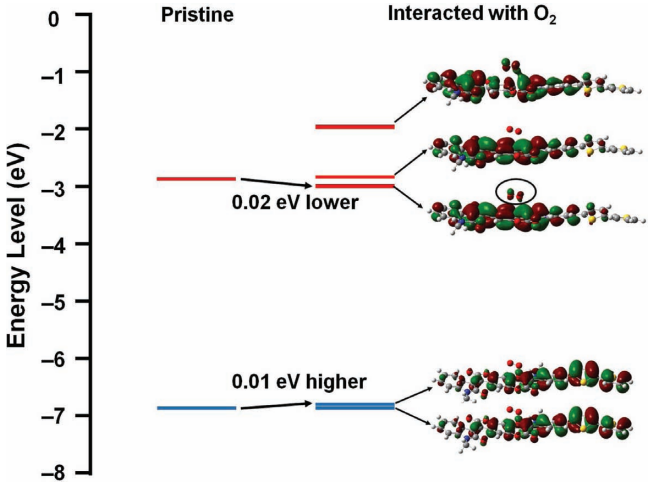

Figure 3. Calculated energy levels and frontier orbitals for the monomer and for the monomer–oxygen complex. Calculations were performed at the M06–2X/6–311G(d,p) level.

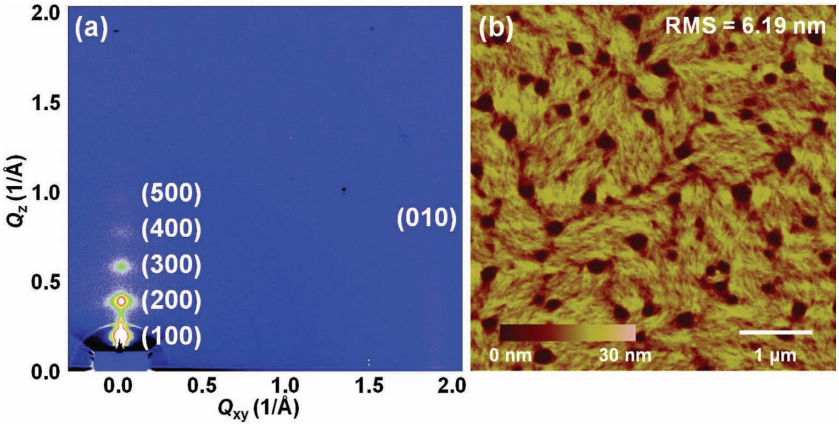

Figure 4. a) 2D-GIXD pattern and b) AFM height image of polymer **BDOPV-2T** film fabricated under the same conditions as the FET device (200 °C annealing).

shallow traps were formed in the polymer film. Furthermore, oxygen also caused the increase of the HOMO level, which would reduce the hole injection barrier from the Au electrode, and therefore increased the hole mobility. Very recently, Sirringhaus et al. found that the HOMO level of polymers slightly increased upon interacting with molecular oxygen,[22] which resulted in hole accumulation in the electrical characteristics. Their results are consistent with our findings and support our hypothesis that the significantly increased hole mobilities were caused by oxygen doping of the polymer in the solid state.

To investigate the film microstructure and morphology, grazing incident X-ray diffraction (GIXD) and tapping-mode atomic force microscopy (AFM) were used (**Figure 4**). The film of **BDOPV-2T** showed a strong out-of-plane diffraction peak (100) at 2θ of 2.48°, corresponding to a *d*-spacing of 28.6 Å (λ = 1.24 Å) (Figure 4a). Another four orders of diffraction peaks attributed to (*h*00) diffractions were also observed, suggesting that a good lamellar edge-on packing occurred in the film. Interestingly, the lamellar distance of 28.6 Å is shorter than the molecular modeled length of the alkyl chains, suggesting that the long alkyl chains were not fully extended in the film. An in-plane (010) peak was also observed, which was attributed to the π–π stacking distance. The measured π–π stacking distance was 3.55 Å, slightly smaller than those of polymers with similar branched alkyl chains.[14] The AFM height image of a **BDOPV-2T** film showed a crystalline fiber-like intercalating network with a relatively high root-mean-square (RMS) deviation of 6.19 nm, presumably due to the strong interchain interactions. These results indicate that **BDOPV-2T** has a strong tendency to crystallize and undergo ordered interchain packing in a film, which may largely contribute to its high charge carrier mobility.[15]

In summary, a novel low-bandgap donor–acceptor polymer **BDOPV-2T** has been developed for high-performance n-type and oxygen-doped ambipolar polymer FETs. The giant aromatic **BDOPV** unit, long branched alkyl chains, centrosymmetric donors, and low-lying LUMO level of the polymer work synergistically to give high electron mobilities up to 1.74 $cm^2\ V^{-1}\ s^{-1}$ under ambient conditions, which is among the highest electron mobilities in both small-molecule and polymer-based FETs.[23] For the ambient-fabricated devices, the hole mobility of **BDOPV-2T** significantly increased to 0.47 $cm^2\ V^{-1}\ s^{-1}$ after oxygen doping, whereas a high electron mobility up to 1.45 $cm^2\ V^{-1}\ s^{-1}$ was still maintained. Furthermore, inverters with high gain values up to 49 are also demonstrated based on the oxygen-doped devices, suggesting the potential application of the polymer in complex logic circuits. Our results represent the first polymer that exhibits electron mobility over 1 $cm^2\ V^{-1}\ s^{-1}$ for devices both fabricated and tested under ambient conditions, thus suggesting promising application of **BDOPV**-based donor–acceptor polymers in semiconducting materials that require both high electron mobility and good ambient stability.

Experimental Section

Synthesis of BDOPV-2T: BDOPV (50 mg, 0.0289 mmol), 5,5′-bis(trimethylstannyl)-2,2′-bithiophene (14.2 mg, 0.0289 mmol), $Pd_2(dba)_3$ (0.5 mg, 2 mol %), P(*o*-tol)$_3$ (0.7 mg, 8 mol %), and 10 mL of toluene were added to a Schlenk tube. The tube was charged with nitrogen through a freeze–pump–thaw cycle three times. The mixture was stirred for 24 h at 120 °C. *N*,*N*′-Diethylphenylazothioformamide (10 mg) was then added and the mixture was stirred for 1 h to remove any residual catalyst before being precipitated into methanol (200 mL). The precipitate was filtered through a nylon filter and purified via Soxhlet extraction for 8 h with acetone, 12 h with hexane, and finally collected with chloroform. The chloroform solution was then concentrated by evaporation and precipitated into methanol (200 mL) and filtered off to afford a dark solid (47 mg, yield 94%).

FET and inverter fabrication and characterization: TG/BC FET devices and complementary inverters were fabricated using n^{++}-Si/SiO_2 (300 nm) substrates. The gold source and drain bottom electrodes (with Ti as the adhesion layer) were patterned by photolithography on the SiO_2 surface. The substrates were subjected to cleaning using ultrasonication in acetone, detergent, deionized water (twice), and isopropyl alcohol. The cleaned substrates were dried under vacuum at 80 °C. All the above processes were performed under ambient conditions. The substrates were transferred into a glovebox (for n-type) or directly used under ambient conditions (for ambipolar). A thin film of the polymer was deposited on the treated substrates by spin-coating at 2000 rpm for 60 s using a polymer solution (3 mg mL^{-1} in DCB), optionally followed by thermal annealing at 140, 160, 180, 200, or 220 °C for 5 min. After the deposition of the polymer thin film, a CYTOP solution (CTL809M:CTsolv180 = 3:1) was spin-coated onto the semiconducting layer at 2000 rpm for 60 s, resulting in a 500 nm thick dielectric layer. The CYTOP layer was then baked at 100 °C for 30 min in a glovebox or under ambient conditions. Gate electrodes comprising a layer of Al (50 nm) were then evaporated through a shadow mask onto the dielectric layer by thermal evaporation under high vacuum (10^{-4} Pa) for both n-type and ambipolar devices. The evaluations of the FETs for both n-type and ambipolar devices and inverters were carried out under ambient conditions (R_H = 40–50%) on a probe stage using a Keithley 4200 SCS as parameter analyzer. The carrier mobility (μ) was calculated from the data in the saturated regime according to the equation $I_{SD} = (W/2L)C_i\mu(V_G - V_T)^2$, where I_{SD} is the drain current in the saturated regime. *W* and *L* are the semiconductor channel width and length, respectively. C_i (C_i = 3.7 nF) is the capacitance per unit area of the gate dielectric layer. V_G and V_T are the gate voltage and threshold voltage, respectively. $V_G - V_T$ of the device was determined from the relationship between the square root of I_{SD} and V_G at the saturated regime.

Supporting Information

Supporting Information is available from the Wiley Online Library or from the author.

Acknowledgements

This work was supported by the Major State Basic Research Development Program (Nos. 2009CB623601 and 2013CB933501) from the Ministry of Science and Technology, and National Natural Science Foundation of China. The authors thank beamline BL14B1 (Shanghai Synchrotron Radiation Facility) for providing the beam time.

Received: May 19, 2013
Revised: July 9, 2013
Published online: August 23, 2013

[1] a) P. F. Moonen, I. Yakimets, J. Huskens, *Adv. Mater.* **2012**, *24*, 5526; b) J. Mei, Y. Diao, A. L. Appleton, L. Fang, Z. Bao, *J. Am. Chem. Soc.* **2013**, *135*, 6724; c) D. Khim, H. Han, K.-J. Baeg, J. Kim, S.-W. Kwak, D.-Y. Kim, Y.-Y. Noh, *Adv. Mater.* **2013**, DOI: 10.1002/adma.201205330.

[2] a) C. B. Nielsen, M. Turbiez, I. McCulloch, *Adv. Mater.* **2013**, *25*, 1859; b) J. D. Yuen, F. Wudl, *Energy Environ. Sci.* **2013**, *6*, 392; c) P. M. Beaujuge, J. M. J. Fréchet, *J. Am. Chem. Soc.* **2011**, *133*, 20009.

[3] A. J. Heeger, *Chem. Soc. Rev.* **2010**, *39*, 2354.

[4] a) H. Chen, Y. Guo, G. Yu, Y. Zhao, J. Zhang, D. Gao, H. Liu, Y. Liu, *Adv. Mater.* **2012**, *24*, 4618; b) J. Li, Y. Zhao, H. S. Tan, Y. Guo, C.-A. Di, G. Yu, Y. Liu, M. Lin, S. H. Lim, Y. Zhou, H. Su, B. S. Ong, *Sci. Rep.* **2012**, *2*, 754; c) Y. Li, S. P. Singh, P. Sonar, *Adv. Mater.* **2010**, *22*, 4862; d) P. Sonar, S. P. Singh, Y. Li, M. S. Soh, A. Dodabalapur, *Adv. Mater.* **2010**, *22*, 5409; e) P. Sonar, T. R. B. Foong, S. P. Singh, Y. Li, A. Dodabalapur, *Chem. Commun.* **2012**, *48*, 8383.

[5] a) S. Wang, M. Kappl, I. Liebewirth, M. Müller, K. Kirchhoff, W. Pisula, K. Müllen, *Adv. Mater.* **2012**, *24*, 417; b) H. N. Tsao, D. M. Cho, I. Park, M. R. Hansen, A. Mavrinskiy, D. Y. Yoon, R. Graf, W. Pisula, H. W. Spiess, K. Müllen, *J. Am. Chem. Soc.* **2011**, *133*, 2605; c) H.-R. Tseng, L. Ying, B. B. Y. Hsu, L. A. Perez, C. J. Takacs, G. C. Bazan, A. J. Heeger, *Nano. Lett.* **2012**, *12*, 6353.

[6] a) T. Lei, J.-H. Dou, Z.-J. Ma, C.-J. Liu, J.-Y. Wang, J. Pei, *Chem. Sci.* **2013**, *4*, 2447; b) T. Lei, J.-H. Dou, Z.-J. Ma, C.-H. Yao, C.-J. Liu, J.-Y. Wang, J. Pei, *J. Am. Chem. Soc.* **2012**, *134*, 20025; c) J. Mei, D. H. Kim, A. L. Ayzner, M. F. Toney, Z. Bao, *J. Am. Chem. Soc.* **2011**, *133*, 20130; d) T. Lei, Y. Cao, Y. Fan, C.-J. Liu, S.-C. Yuan, J. Pei, *J. Am. Chem. Soc.* **2011**, *133*, 6099.

[7] a) H. Huang, Z. Chen, R. P. Ortiz, C. Newman, H. Usta, S. Lou, J. Youn, Y.-Y. Noh, K.-J. Baeg, L. X. Chen, A. Facchetti, T. Marks, *J. Am. Chem. Soc.* **2012**, *134*, 10966; b) K.-J. Baeg, D. Khim, S.-W. Jung, M. Kang, I.-K. You, D.-Y. Kim, A. Facchetti, Y.-Y. Noh, *Adv. Mater.* **2012**, *24*, 5433.

[8] a) J. Fan, J. D. Yuen, W. Cui, J. Seifter, A. R. Mohebbi, M. Wang, H. Zhou, A. Heeger, F. Wudl, *Adv. Mater.* **2012**, *24*, 6164; b) J. Fan, J. D. Yuen, M. Wang, J. Seifter, J.-H. Seo, A. R. Mohebbi, D. Zakhidov, A. Heeger, F. Wudl, *Adv. Mater.* **2012**, *24*, 2186; c) J. D. Yuen, J. Fan, J. Seifter, B. Lim, R. Hufschmid, A. J. Heeger, F. Wudl, *J. Am. Chem. Soc.* **2011**, *133*, 20799.

[9] a) J. H. Park, E. H. Jung, J. W. Jung, W. H. Jo, *Adv. Mater.* **2013**, *25*, 2583; b) C. Kanimozhi, N. Yaacobi-Gross, K. W. Chou, A. Amassian, T. D. Anthopoulos, S. Patil, *J. Am. Chem. Soc.* **2012**, *134*, 16532.

[10] a) H. Yan, Z. Chen, Y. Zheng, C. Newman, J. R. Quinn, F. Dotz, M. Kastler, A. Facchetti, *Nature* **2009**, *457*, 679; b) H. Usta, C. Newman, Z. Chen, A. Facchetti, *Adv. Mater.* **2012**, *24*, 3678; c) X. Zhan, A. Facchetti, S. Barlow, T. J. Marks, M. A. Ratner, M. R. Wasielewski, S. R. Marder, *Adv. Mater.* **2011**, *23*, 268; d) A. Babel, S. A. Jenekhe, *J. Am. Chem. Soc.* **2003**, *125*, 13656.

[11] R. Di Pietro, H. Sirringhaus, *Adv. Mater.* **2012**, *24*, 3367.

[12] a) C. Wang, H. Dong, W. Hu, Y. Liu, D. Zhu, *Chem. Rev.* **2011**, *112*, 2208; b) V. Coropceanu, J. Cornil, D. A. da Silva Filho, Y. Olivier, R. Silbey, J.-L. Brédas, *Chem. Rev.* **2007**, *107*, 926.

[13] T. Lei, J.-H. Dou, X.-Y. Cao, J.-Y. Wang, J. Pei, *J. Am. Chem. Soc.* **2013**, DOI: 10.1021/ja403624a.

[14] T. Lei, J.-H. Dou, J. Pei, *Adv. Mater.* **2012**, *24*, 6457.

[15] T. Lei, Y. Cao, X. Zhou, Y. Peng, J. Bian, J. Pei, *Chem. Mater.* **2012**, *24*, 1762.

[16] During the preparation of this manuscript, Li et al. independently reported two structurally similar **BDOPV**-based donor–acceptor polymers. Z. Yan, B. Sun, Y. Li, *Chem. Commun.* **2013**, *49*, 3790.

[17] C.-A. Di, Y. Liu, G. Yu, D. Zhu, *Acc. Chem. Res.* **2009**, *42*, 1573.

[18] a) Z. Chen, M. J. Lee, R. Shahid Ashraf, Y. Gu, S. Albert-Seifried, M. Meedom Nielsen, B. Schroeder, T. D. Anthopoulos, M. Heeney, I. McCulloch, H. Sirringhaus, *Adv. Mater.* **2012**, *24*, 647; b) Z. Chen, H. Lemke, S. Albert-Seifried, M. Caironi, M. M. Nielsen, M. Heeney, W. Zhang, I. McCulloch, H. Sirringhaus, *Adv. Mater.* **2010**, *22*, 2371.

[19] a) P. G. Collins, K. Bradley, M. Ishigami, A. Zettl, *Science* **2000**, *287*, 1801; b) S. Ryu, L. Liu, S. Berciaud, Y.-J. Yu, H. Liu, P. Kim, G. W. Flynn, L. E. Brus, *Nano. Lett.* **2010**, *10*, 4944.

[20] H. Okamoto, N. Kawasaki, Y. Kaji, Y. Kubozono, A. Fujiwara, M. Yamaji, *J. Am. Chem. Soc.* **2008**, *130*, 10470.

[21] Y. Wang, S. D. Motta, F. Negri, R. Friedlein, *J. Am. Chem. Soc.* **2011**, *133*, 10054.

[22] R. Di Pietro, D. Fazzi, T. B. Kehoe, H. Sirringhaus, *J. Am. Chem. Soc.* **2012**, *134*, 14877.

[23] a) J. Lee, A-R. Han, J. Kim, Y. Kim, J. H. Oh, C. Yang, *J. Am. Chem. Soc.* **2012**, *134*, 20713; b) Y. Hu, Q. Lu, H. Li, N. Zhang, X. Liu, *Appl. Phys. Express* **2013**, *6*, 051602; c) S. Z. Bisri, T. Takenobu, Y. Yomogida, H. Shimotani, T. Yamao, S. Hotta, Y. Iwasa, *Adv. Funct. Mater.* **2009**, *19*, 1728; d) S. Z. Bisri, T. Takenobu, T. Takahashi, Y. Iwasa, *Appl. Phys. Lett.* **2010**, *96*, 183304; e) H. Nakanotani, M. Saito, H. Nakamura, C. Adachi, *Appl. Phys. Lett.* **2009**, *95*, 103307.